AXISYMMETRIC FINITE ELASTICITY

by
Stephen V. Harren
http://www.harren.us

CONTENTS

1. The Two-Dimensional Eigenproblem

In cylindrical coordinates (r, z, θ) for axisymmetric problems, tensorial quantities which reside in the rz–plane are two-dimensional Cartesian tensors.

Consider a symmetric, second-order tensor in the rz–plane $\mathbf{A}$ such that

$$A = \begin{bmatrix} A_{00} & A_{01} \\ A_{01} & A_{11} \end{bmatrix} , \qquad A^E = \begin{bmatrix} \lambda_0 & 0 \\ 0 & \lambda_1 \end{bmatrix} , \qquad A^E = \psi A \psi^T , \qquad A = \psi^T A^E \psi , \tag{1.1}$$

where

$$\psi = \begin{bmatrix} \cos\alpha & \sin\alpha \\ -\sin\alpha & \cos\alpha \end{bmatrix} , \qquad \mathbf{e}_i^E = \psi_{ij}\mathbf{e}_j . \tag{1.2}$$

In eqns. (1.1) and (1.2), λ_i are the eigenvalues of $\mathbf{A}$, $\mathbf{e}_i^E$ are the corresponding eigenvectors, and $\mathbf{e}_i$ are the base vectors in the rz–plane, *i.e.,* this is the standard two-dimensional eigenproblem. Using the third of eqns. (1.1),

$$A_{01}^E = 0 = \frac{1}{2}(A_{11} - A_{00})\sin 2\alpha + A_{01}\cos 2\alpha \quad \Rightarrow \quad \alpha = \frac{1}{2}\tan^{-1}\left(\frac{2A_{01}}{A_{00} - A_{11}}\right) , \tag{1.3}$$

which solves for the eigenvectors. The third of eqns. (1.1) also yields the eigenvalues

$$\lambda_0 = A_{00}^E = \frac{1}{2}(A_{00} + A_{11}) - \frac{1}{2}(A_{11} - A_{00})\cos 2\alpha + A_{01}\sin 2\alpha ,$$
$$\lambda_1 = A_{11}^E = \frac{1}{2}(A_{00} + A_{11}) + \frac{1}{2}(A_{11} - A_{00})\cos 2\alpha - A_{01}\sin 2\alpha . \tag{1.4}$$

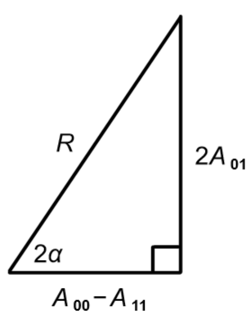

Figure 1. Right triangle corresponding to the last of eqns. (1.3).

In a numerical method, the gradients of the eigenproblem with respect to A_{ij} are required. Consequently, differentiation of the last of eqns. (1.3) gives

$$\frac{\partial\alpha}{\partial A_{00}} = -\frac{A_{01}}{(A_{00} - A_{11})^2 + 4A_{01}^2} ,$$
$$\frac{\partial\alpha}{\partial A_{01}} = \frac{A_{00} - A_{11}}{(A_{00} - A_{11})^2 + 4A_{01}^2} , \tag{1.5}$$
$$\frac{\partial\alpha}{\partial A_{11}} = \frac{A_{01}}{(A_{00} - A_{11})^2 + 4A_{01}^2} .$$

Next, using the right triangle in Fig. 1 above, eqns. (1.5) may be simplified as

$$\frac{\partial\alpha}{\partial A_{00}} = -\frac{\sin 2\alpha}{2R} , \qquad \frac{\partial\alpha}{\partial A_{01}} = \frac{\cos 2\alpha}{R} , \qquad \frac{\partial\alpha}{\partial A_{11}} = \frac{\sin 2\alpha}{2R} , \tag{1.6}$$

where

$$R = \sqrt{(A_{00} - A_{11})^2 + 4A_{01}^2} . \tag{1.7}$$

Now, differentiating eqns. (1.4) with respect to A_{kl}, and using the first of eqns. (1.3), one obtains

$$\frac{\partial\lambda_0}{\partial A_{00}} = \frac{1}{2}(1 + \cos 2\alpha) , \qquad \frac{\partial\lambda_0}{\partial A_{11}} = \frac{1}{2}(1 - \cos 2\alpha) , \qquad \frac{\partial\lambda_0}{\partial A_{01}} = \sin 2\alpha ,$$

$$\frac{\partial\lambda_1}{\partial A_{00}} = \frac{1}{2}(1-\cos 2\alpha) \ , \qquad \frac{\partial\lambda_1}{\partial A_{11}} = \frac{1}{2}(1+\cos 2\alpha) \ , \qquad \frac{\partial\lambda_1}{\partial A_{01}} = -\sin 2\alpha \ . \tag{1.8}$$

Finally, differentiating the eigenvectors (1.2) gives

$$\frac{\partial\psi_{ij}}{\partial\alpha} = \begin{bmatrix} -\sin\alpha & \cos\alpha \\ -\cos\alpha & -\sin\alpha \end{bmatrix} \ , \qquad \frac{\partial\psi_{ij}}{\partial A_{kl}} = \frac{\partial\psi_{ij}}{\partial\alpha}\frac{\partial\alpha}{\partial A_{kl}} \ , \tag{1.9}$$

where $\partial\alpha/\partial A_{kl}$ are as per eqn. (1.6). Thus, the gradients of the eigenproblem are given by eqns. (1.8) and (1.9).

2. Two-Dimensional Strain Measures

The Polar Decomposition Theorem states that

$$F = VR \ , \tag{2.1}$$

where F is the deformation gradient, V is the (symmetric) left stretch tensor (with positive eigenvalues), and R is the rotation tensor. Consider

$$B = FF^T = VRR^TV = VIV = VV \quad \Rightarrow \quad V = \sqrt{B} \ . \tag{2.2}$$

The square root is calculated by way of the two-dimensional eigenproblem, *viz.,*

$$B = \begin{bmatrix} B_{00} & B_{01} \\ B_{01} & B_{11} \end{bmatrix} \ , \qquad B^E = \begin{bmatrix} \lambda_0 & 0 \\ 0 & \lambda_1 \end{bmatrix} \ , \qquad B^E = \psi B \psi^T \ , \tag{2.3}$$

so that

$$V^E = \begin{bmatrix} \sqrt{\lambda_0} & 0 \\ 0 & \sqrt{\lambda_1} \end{bmatrix} \ , \qquad V = \psi^T V^E \psi \ . \tag{2.4}$$

For a numerical method, the gradients $\partial V_{ij}/\partial F_{pq}$ are needed. Consequently, differentiation of $B = VV$ gives

$$\frac{\partial B_{ij}}{\partial V_{pq}} = I_{ikpq}V_{kj} + V_{ik}I_{kjpq} \ , \tag{2.5}$$

where I_{ijkl} is the fully symmetric fourth-order identity tensor, *i.e.,*

$$I_{ijkl} = \frac{1}{2}\left(\delta_{ik}\delta_{jl} + \delta_{jk}\delta_{il}\right) \ , \tag{2.6}$$

and δ_{ij} is the two-dimensional identity matrix (or Kronecker delta). But, $\partial V_{ij}/\partial B_{kl}$ is required, which satisfies the inverse relation

$$\frac{\partial B_{ij}}{\partial V_{kl}}\frac{\partial V_{kl}}{\partial B_{mn}} = I_{ijmn} \ , \tag{2.7}$$

and which can be written out in the matrix form

$$\begin{bmatrix} \frac{\partial B_{00}}{\partial V_{00}} & 2\frac{\partial B_{00}}{\partial V_{01}} & \frac{\partial B_{00}}{\partial V_{11}} \\ 2\frac{\partial B_{01}}{\partial V_{00}} & 4\frac{\partial B_{01}}{\partial V_{01}} & 2\frac{\partial B_{01}}{\partial V_{11}} \\ \frac{\partial B_{11}}{\partial V_{00}} & 2\frac{\partial B_{11}}{\partial V_{01}} & \frac{\partial B_{11}}{\partial V_{11}} \end{bmatrix} \begin{bmatrix} \frac{\partial V_{00}}{\partial B_{00}} & \frac{\partial V_{00}}{\partial B_{01}} & \frac{\partial V_{00}}{\partial B_{11}} \\ \frac{\partial V_{01}}{\partial B_{00}} & \frac{\partial V_{01}}{\partial B_{01}} & \frac{\partial V_{01}}{\partial B_{11}} \\ \frac{\partial V_{11}}{\partial B_{00}} & \frac{\partial V_{11}}{\partial B_{01}} & \frac{\partial V_{11}}{\partial B_{11}} \end{bmatrix} = \begin{bmatrix} 1 & 0 & 0 \\ 0 & 1 & 0 \\ 0 & 0 & 1 \end{bmatrix} . \tag{2.8}$$

Thus, the calculation of $\partial V_{ij}/\partial B_{kl}$ amounts to inverting a 3×3 matrix. Next, differentiation of $B = FF^T$ yields

$$\frac{\partial B_{ij}}{\partial F_{pq}} = \delta_{ip} F_{jq} + F_{iq} \delta_{jp} \ . \tag{2.9}$$

Finally, by the Chain Rule,

$$\frac{\partial V_{ij}}{\partial F_{pq}} = \frac{\partial V_{ij}}{\partial B_{kl}} \frac{\partial B_{kl}}{\partial F_{pq}} \ . \tag{2.10}$$

For finite elasticity, the most appropriate strain measure is the logarithmic (or true) strain ε, defined by

$$\varepsilon = \ln V \ . \tag{2.11}$$

Once again, the logarithm is calculated via the two-dimensional eigenproblem. Thus,

$$V = \begin{bmatrix} V_{00} & V_{01} \\ V_{01} & V_{11} \end{bmatrix} , \qquad V^E = \begin{bmatrix} \lambda_0 & 0 \\ 0 & \lambda_1 \end{bmatrix} , \qquad V^E = \psi V \psi^T \ , \tag{2.12}$$

with

$$\varepsilon^E = \begin{bmatrix} \ln \lambda_0 & 0 \\ 0 & \ln \lambda_1 \end{bmatrix} , \qquad \varepsilon = \psi^T \varepsilon^E \psi \ . \tag{2.13}$$

The gradients $\partial \varepsilon_{kl}/\partial V_{pq}$ are obtained by differentiating the second of eqns. (2.13), *viz.,*

$$\frac{\partial \varepsilon_{kl}}{\partial V_{pq}} = \frac{\partial \varepsilon_{ij}^E}{\partial V_{pq}} \psi_{ik} \psi_{jl} + \varepsilon_{ij}^E \frac{\partial \psi_{ik}}{\partial V_{pq}} \psi_{jl} + \varepsilon_{ij}^E \psi_{ik} \frac{\partial \psi_{jl}}{\partial V_{pq}} \ , \tag{2.14}$$

where

$$\frac{\partial \varepsilon_{ij}^E}{\partial V_{pq}} = \begin{bmatrix} \dfrac{1}{\lambda_0} \dfrac{\partial \lambda_0}{\partial V_{pq}} & 0 \\ 0 & \dfrac{1}{\lambda_1} \dfrac{\partial \lambda_1}{\partial V_{pq}} \end{bmatrix} . \tag{2.15}$$

Note that the derivatives $\partial \lambda_i/\partial V_{pq}$ and $\partial \psi_{ij}/\partial V_{pq}$ are listed in, respectively, eqns. (1.8) and (1.9) with V_{ij} replacing A_{ij}.

3. Axisymmetric Strain Measures

For axisymmetric problems in cylindrical coordinates (r, z, θ), the deformation gradient component $F_{\theta\theta} = F_{22} = 1 + u_r/r$, where u_r is the radial displacement, and r is the radial coordinate in the undeformed configuration. Also, any derivatives with respect to θ are zero. Notwithstanding, for axisymmetric problems, the deformation gradient F and left stretch tensor V are of the form

$$F = \begin{bmatrix} F_{00} & F_{01} & 0 \\ F_{10} & F_{11} & 0 \\ 0 & 0 & F_{22} \end{bmatrix} , \qquad V = \begin{bmatrix} V_{00} & V_{01} & 0 \\ V_{01} & V_{11} & 0 \\ 0 & 0 & F_{22} \end{bmatrix} . \tag{3.1}$$

Note that the formulas for V_{ij} $(i, j) \in (0,1)$ are as given above in eqn. (2.4). Also, the formulas for $\partial V_{ij}/\partial F_{pq}$ $(i, j, p, q) \in (0,1)$ are as per eqn. (2.10). All other values of $\partial V_{ij}/\partial F_{pq}$ are zero, except for $\partial V_{22}/\partial F_{22} = 1$.

As for the logarithmic strain,

$$\varepsilon = \begin{bmatrix} \varepsilon_{00} & \varepsilon_{01} & 0 \\ \varepsilon_{01} & \varepsilon_{11} & 0 \\ 0 & 0 & \varepsilon_{22} \end{bmatrix} , \qquad \varepsilon_{22} = \ln V_{22} = \ln F_{22} \ . \tag{3.2}$$

As before, the formulas for ε_{ij} $(i,j) \in (0,1)$ are given by the two-dimensional case, *cf.*, eqn. (2.13), and the derivatives $\partial\varepsilon_{ij}/\partial V_{pq}$ $(i,j,p,q) \in (0,1)$ are as per eqn. (2.14). All other $\partial\varepsilon_{ij}/\partial V_{pq}$ are zero, except for $\partial\varepsilon_{22}/\partial V_{22} = 1/V_{22}$.

4. Uniaxial Finite Elastic Response

Figure 2 below shows the uniaxial stress-strain curve for vulcanized rubber. The blue plotted points in the figure are the experimental data of Treloar (1940), see the "Herve Marand Rubber Elasticity Lecture 17" (`eng.uc.edu`). While the author is not quite sure of the exact meaning of σ and ε in the figure, herein they will be interpreted as being true stress and true (or logarithmic) strain. The red curve in the figure is a piecewise cubic fit to the data, which fit is constructed as follows. The ε–axis is broken into n subintervals, the ith one of which is depicted below in Fig. 3. The normalized coordinate $\xi \in (-1,1)$ in the figure is

$$\xi = \frac{2\varepsilon - \varepsilon^{i+1} - \varepsilon^{i}}{L} \ , \qquad L = \varepsilon^{i+1} - \varepsilon^{i} \ . \tag{4.1}$$

Now, in each subinterval $i \in (0, n-2)$, the uniaxial stress is written as

$$\sigma = a^0\sigma^i + a^1 m^i + a^2\sigma^{i+1} + a^3 m^{i+1} \ , \tag{4.2}$$

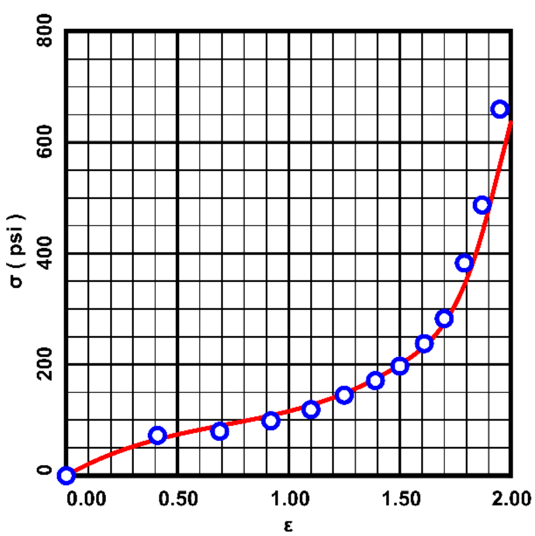

Figure 2. Stress-strain data for vulcanized rubber as explained in the text.

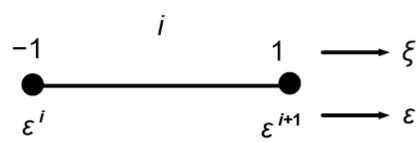

Figure 3. Normalized subinterval.

where, *e.g.*, m^i is the slope of the stress-strain curve at point i in Fig. 3, and

$$\begin{aligned} a^0 &= \frac{1}{4}(2 - 3\xi + \xi^3) \ , \\ a^1 &= \frac{L}{8}(1 - \xi - \xi^2 + \xi^3) \ , \\ a^2 &= \frac{1}{4}(2 + 3\xi - \xi^3) \ , \\ a^3 &= \frac{L}{8}(-1 - \xi + \xi^2 + \xi^3) \ . \end{aligned} \tag{4.3}$$

The derivative of eqn. (4.2) is

$$\frac{\mathrm{d}\sigma}{\mathrm{d}\varepsilon} = a^0_{,\varepsilon}\sigma^i + a^1_{,\varepsilon} m^i + a^2_{,\varepsilon}\sigma^{i+1} + a^3_{,\varepsilon} m^{i+1} \, , \tag{4.4}$$

with

$$a^0_{,\varepsilon} = \frac{3}{2L}(-1+\xi^2) \ , \qquad a^1_{,\varepsilon} = \frac{1}{4}(-1-2\xi+3\xi^2) \ ,$$

$$a^2_{,\varepsilon} = \frac{3}{2L}(1-\xi^2) \ , \qquad a^3_{,\varepsilon} = \frac{1}{4}(-1+2\xi+3\xi^2) \ . \tag{4.5}$$

Finally, for the last subinterval $i = n-1$ (*i.e.,* for $\varepsilon > \varepsilon^{n-1}$), the response is taken as linear, *viz.,*

$$\sigma = m^{n-1}(\varepsilon - \varepsilon^{n-1}) + \sigma^{n-1} \ , \qquad \frac{\mathrm{d}\sigma}{\mathrm{d}\varepsilon} = m^{n-1} \ . \tag{4.6}$$

Thus, the red curve in Fig. 2 above is constructed with $n = 3$ and the constants

$$\begin{array}{lll} \varepsilon^0 = 0 \ , & \varepsilon^1 = 1.5 \ , & \varepsilon^2 = 1.9 \\ \sigma^0 = 0 \text{ psi} \ , & \sigma^1 = 200 \text{ psi} \ , & \sigma^2 = 460 \text{ psi} \ , \\ m^0 = 230 \text{ psi} \ , & m^1 = 260 \text{ psi} \ , & m^2 = 1570 \text{ psi} \ . \end{array} \tag{4.7}$$

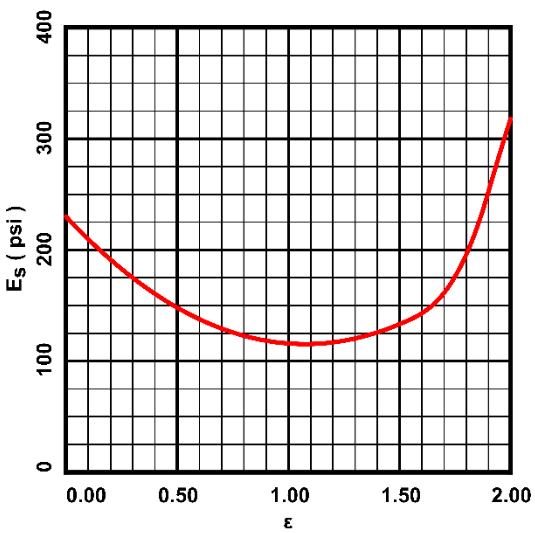

Figure 4. The secant modulus E_s.

Additionally, the secant modulus is

$$E_s = \frac{\sigma}{\varepsilon} \ , \tag{4.8}$$

which is graphed at right in Fig. 4. Finally, differentiation of eqn. (4.8) yields

$$\frac{\mathrm{d}E_s}{\mathrm{d}\varepsilon} = \frac{1}{\varepsilon}\left(\frac{\mathrm{d}\sigma}{\mathrm{d}\varepsilon} - E_s\right) \ . \tag{4.9}$$

5. Multiaxial Response and Stress Measures

Unlike in the previous sections, here the tensor indices range over three dimensions, *i.e.,* $(0,1,2)$ or (r, z, θ), even though the strain components $\varepsilon_{02} = \varepsilon_{20} = \varepsilon_{12} = \varepsilon_{21} = 0$, *cf.,* the first of eqns. (3.2).

Consider a state of tensile uniaxial stress σ_{zz} and uniform deformation so that the strains are ε_{zz} and $\varepsilon_{rr} = \varepsilon_{\theta\theta} = -\nu\varepsilon_{zz}$, where ν is Poisson's ratio. Now, the effective strain $\bar{\varepsilon}$ defined by

$$\bar{\varepsilon} = \sqrt{\frac{\varepsilon_{ij}\varepsilon_{ij}}{1+2\nu^2}} \tag{5.1}$$

is such that, in this case, $\bar{\varepsilon}$ corresponds to the major strain component ε_{zz}. Consequently, eqn. (5.1) can be used to generalize the uniaxial response of Sec. 4 to general states of deformation.

For linear elasticity, the stresses σ_{ij} are related to the strains by Hooke's Law, *i.e.,*

$$\sigma_{ij} = C^0_{ijkl}\varepsilon_{kl} \ , \qquad C^0_{ijkl} = \frac{E}{(1+\nu)(1-2\nu)}\left[\,(1-2\nu)I_{ijkl} + \nu\delta_{ij}\delta_{kl}\,\right] \ , \tag{5.2}$$

where E is Young's modulus. Consistent with the axisymmetric strain state (3.2) and with eqn. (5.2), the axisymmetric stress state is also of the form

$$\sigma = \begin{bmatrix} \sigma_{00} & \sigma_{01} & 0 \\ \sigma_{01} & \sigma_{11} & 0 \\ 0 & 0 & \sigma_{22} \end{bmatrix} \ . \tag{5.3}$$

For axisymmetric finite elasticity, the true stress components σ_{ij} also follow eqn. (5.3).

A reasonable extension of eqn. (5.2) to nonlinear elasticity is to use

$$\sigma_{ij} = C_{ijkl}\varepsilon_{kl} \ , \qquad C_{ijkl} = \frac{E_s}{(1+\nu)(1-2\nu)}\left[\,(1-2\nu)I_{ijkl} + \nu\delta_{ij}\delta_{kl}\,\right] \ , \tag{5.4}$$

where the secant modulus $E_s = \sigma/\bar{\varepsilon}$, *cf.,* eqn. (4.8). In other words, $\sigma = \sigma(\varepsilon)$ in Sec. 4 is generalized to $\sigma = \sigma(\bar{\varepsilon})$. In eqn. (5.4), σ_{ij} are the components of the true stress, and ε_{kl} are the components of the logarithmic strain. Also herein, ν is assumed to be constant (and for the numerical calculations presented later in Sec. 10, $\nu = 0.45$ is used). Finally, it is worth noting that the stress component σ_{ij} is the force per unit deformed area acting in the j–direction of the deformed configuration on a (differential) face whose normal is in the i–direction of the deformed configuration.

In the numerical calculations which follow later, the derivatives $\partial\sigma_{ij}/\partial\varepsilon_{pq}$ are needed. So, differentiation of eqn. (5.1) gives

$$\frac{\partial\bar{\varepsilon}}{\partial\varepsilon_{pq}} = \frac{\varepsilon_{pq}}{(1+2\nu^2)\bar{\varepsilon}} \ . \tag{5.5}$$

Next,

$$\frac{\partial E_s}{\partial\varepsilon_{pq}} = \frac{\mathrm{d}E_s}{\mathrm{d}\bar{\varepsilon}}\frac{\partial\bar{\varepsilon}}{\partial\varepsilon_{pq}} = \frac{1}{(1+2\nu^2)\bar{\varepsilon}^2}\left(\frac{\mathrm{d}\sigma}{\mathrm{d}\bar{\varepsilon}} - E_s\right)\varepsilon_{pq} \ , \tag{5.6}$$

cf., eqn. (4.9). Now,

$$\frac{\mathrm{d}C_{ijkl}}{\mathrm{d}\bar{\varepsilon}} = \frac{1}{\sigma}\left(\frac{\mathrm{d}\sigma}{\mathrm{d}\bar{\varepsilon}} - E_s\right)C_{ijkl} \quad \Rightarrow \quad \frac{\partial C_{ijkl}}{\partial\varepsilon_{pq}} = \frac{\mathrm{d}C_{ijkl}}{\mathrm{d}\bar{\varepsilon}}\frac{\partial\bar{\varepsilon}}{\partial\varepsilon_{pq}} = \frac{1}{(1+2\nu^2)\sigma\bar{\varepsilon}}\left(\frac{\mathrm{d}\sigma}{\mathrm{d}\bar{\varepsilon}} - E_s\right)C_{ijkl}\varepsilon_{pq} \ . \tag{5.7}$$

Finally, differentiation of the first of eqns. (5.4) yields

$$\frac{\partial\sigma_{ij}}{\partial\varepsilon_{pq}} = C_{ijpq} + \frac{\partial C_{ijkl}}{\partial\varepsilon_{pq}}\varepsilon_{kl} \ , \tag{5.8}$$

so that via the second of eqns. (5.7),

$$\frac{\partial\sigma_{ij}}{\partial\varepsilon_{pq}} = C_{ijpq} + \frac{1}{(1+2\nu^2)\sigma\bar{\varepsilon}}\left(\frac{\mathrm{d}\sigma}{\mathrm{d}\bar{\varepsilon}} - E_s\right)\sigma_{ij}\varepsilon_{pq} \ . \tag{5.9}$$

Turning attention now to the nominal stress N_{ij}, which component is the force per unit undeformed area acting on the face whose normal is in the i–direction in the undeformed configuration, with the force acting in the j–direction of the deformed configuration. The nominal stress is given by

$$N_{ij} = (\det F) F_{ik}^{-1} \sigma_{kj} \ . \tag{5.10}$$

Note that, for axisymmetric problems, N additionally is of the form

$$N = \begin{bmatrix} N_{00} & N_{01} & 0 \\ N_{10} & N_{11} & 0 \\ 0 & 0 & N_{22} \end{bmatrix} . \tag{5.11}$$

Now, for square matrices in general,

$$\frac{\partial(\det A)}{\partial A_{pq}} = (\det A) A_{pq}^{-T} \ , \qquad \frac{\partial A_{ik}^{-1}}{\partial A_{pq}} = -A_{ip}^{-1} A_{qk}^{-1} \ . \tag{5.12}$$

Thus, with these, the derivative of eqn. (5.10) is

$$\frac{\partial N_{ij}}{\partial F_{pq}} = F_{qp}^{-1} N_{ij} - F_{ip}^{-1} N_{qj} + (\det F) F_{ik}^{-1} \frac{\partial \sigma_{kj}}{\partial F_{pq}} \ , \tag{5.13}$$

where, by the Chain Rule,

$$\frac{\partial \sigma_{kj}}{\partial F_{pq}} = \frac{\partial \sigma_{kj}}{\partial \varepsilon_{mn}} \frac{\partial \varepsilon_{mn}}{\partial V_{rs}} \frac{\partial V_{rs}}{\partial F_{pq}} \ . \tag{5.14}$$

6. The Principle of Virtual Work

Here we revert to having the tensor indices range over $(0,1)$ or (r, z). Notwithstanding, for axisymmetric problems, equilibrium, in terms of the nominal stress, is

$$N_{ji,j} + f_i = 0 \ , \qquad f_i = \frac{1}{r} \begin{bmatrix} N_{00} - N_{22} \\ N_{01} \end{bmatrix} , \tag{6.1}$$

where the comma denotes differentiation with respect to the coordinates in the undeformed configuration, and r is the radial coordinate in the undeformed configuration. Now, multiply eqn. (6.1) by a once differentiable vector field u_i^* (the virtual displacement) to obtain

$$u_i^* N_{ji,j} + u_i^* f_i = 0 \ . \tag{6.2}$$

By the product rule of differentiation $\left(u_i^* N_{ji}\right)_{,j} = u_{i,j}^* N_{ji} + u_i^* N_{ji,j}$, which when put into eqn. (6.2) yields

$$u_{i,j}^* N_{ji} - u_i^* f_i = \left(u_i^* N_{ji}\right)_{,j} \ . \tag{6.3}$$

Next, integrate eqn. (6.3) over the volume of the body V, and use the Divergence Theorem to get

$$\int_V u_{i,j}^* N_{ji} \mathrm{d}V - \int_V u_i^* f_i \mathrm{d}V = \int_S u_i^* T_i \mathrm{d}S \ , \tag{6.4}$$

which is the Principle of Virtual Work. In eqn. (6.4), S is the bounding surface of the body, and $T_i = n_j N_{ji}$ is the nominal traction vector (**n** is the outward-pointing unit normal vector on S).

Introduce the finite element nodal shape functions S^I, and interpolate the virtual displacement through the element via

$$u_i^* = S^I u_i^{*I} \ , \qquad u_{i,j}^* = S_{,j}^I u_i^{*I} \ , \tag{6.5}$$

where u_i^{*I} are the nodal values of the virtual displacement. With these interpolations, eqn. (6.4) becomes

$$u_i^{*I}\int\limits_V S^I_{,j}N_{ji}\mathrm{d}V - u_i^{*I}\int\limits_V S^I f_i\mathrm{d}V = u_i^{*I}\int\limits_S S^I T_i\mathrm{d}S \ , \tag{6.6}$$

or since u_i^{*I} is arbitrary,

$$\int\limits_V S^I_{,j}N_{ji}\mathrm{d}V - \int\limits_V S^I f_i\mathrm{d}V = \int\limits_S S^I T_i\mathrm{d}S \ . \tag{6.7}$$

Equation (6.7) is the basis of the finite element method.

7. The Four-Noded Isoparametric Finite Element

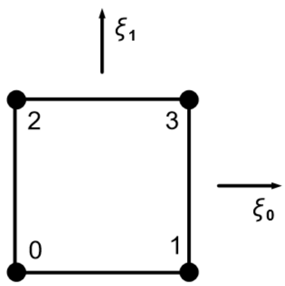

Figure 5. Four-noded element in **ξ**–space.

At left, in Fig. 5, is shown the four-noded finite element in **ξ**–space, where $\xi_i \in (-1,1)$. With

$$f^0(s) = \frac{1}{2}(1-s) \ , \qquad f^1(s) = \frac{1}{2}(1+s) \ , \tag{7.1}$$

the four shape functions S^I are given by the tensor product

$$S^0 = f^0(\xi_0)f^0(\xi_1) \ , \qquad S^1 = f^1(\xi_0)f^0(\xi_1) \ ,$$
$$S^2 = f^0(\xi_0)f^1(\xi_1) \ , \qquad S^3 = f^1(\xi_0)f^1(\xi_1) \ . \tag{7.2}$$

The mapping to **x**–space is accomplished via

$$x_i = S^I x_i^I \ , \tag{7.3}$$

where $(x_0, x_1) = (r, z)$ and x_i^I are the nodal coordinates. The differential of eqn. (7.3) is

$$\mathrm{d}x_i = A_{i\alpha}\mathrm{d}\xi_\alpha \ , \qquad A_{i\alpha} = \frac{\partial x_i}{\partial \xi_\alpha} = S^I_{,\alpha}x_i^I \ , \qquad \mathrm{d}\xi_\alpha = A^{-1}_{\alpha i}\mathrm{d}x_i \ , \qquad A^{-1}_{\alpha i} = \frac{\partial \xi_\alpha}{\partial x_i} \ . \tag{7.4}$$

By the chain rule and eqns. (7.4), the gradients of the shape functions in **x**–space are

$$S^I_{,i} = S^I_{,\alpha}A^{-1}_{\alpha i} \ . \tag{7.5}$$

Also consistent with eqns. (7.4),

$$\mathrm{d}A^{\mathbf{x}} = \mathrm{d}r\mathrm{d}z = (\det A)\mathrm{d}A^{\boldsymbol{\xi}} \ , \qquad dV = 2\pi r\mathrm{d}r\mathrm{d}z = 2\pi r(\det A)\mathrm{d}A^{\boldsymbol{\xi}} \ , \qquad \mathrm{d}A^{\boldsymbol{\xi}} = \mathrm{d}\xi_0\mathrm{d}\xi_1 \ . \tag{7.6}$$

Thus, volume integrals are transformed as

$$\int\limits_V (\ )dV = \int\limits_{-1}^{1}\int\limits_{-1}^{1} (\ )2\pi r(\det A)\, d\xi_0 d\xi_1 \ . \tag{7.7}$$

In a finite element program, the integration on the right side of eqn. (7.7) is performed numerically with the 3–point Gauss-Legendre quadrature rule, which rule integrates a fifth-order polynomial exactly.

8. Linear Elastic Finite Element Equations

The initial guess for the solution to the first nonlinear load step is a linear elastic solution. For linear elasticity then, eqn. (6.7) is

$$\int_V S^I_{,j}\sigma_{ji}\mathrm{d}V - \int_V S^I f_i \mathrm{d}V = \int_S S^I T_i \mathrm{d}S \ , \qquad f_i = \frac{1}{r}\begin{bmatrix} \sigma_{00} - \sigma_{22} \\ \sigma_{01} \end{bmatrix} . \tag{8.1}$$

Now, since the strain component $\varepsilon_{22} = \varepsilon_{\theta\theta} = (1/r)u_r$, write Hooke's Law (5.2) as

$$\sigma_{ij} = C^0_{ijkl}u_{l,k} + \frac{1}{r}C^0_{ij22}u_r \ , \qquad \sigma_{22} = C^0_{22kl}u_{l,k} + \frac{1}{r}C^0_{2222}u_r \ . \tag{8.2}$$

Next, interpolate the displacement field through the element via

$$u_l = S^J u^J_l \ , \qquad u_{l,k} = S^J_{,k}u^J_l \ , \qquad u_0 = u_r = [\, S^J \quad 0 \,]\begin{bmatrix} u^J_0 \\ u^J_1 \end{bmatrix} = T^J_l u^J_l \ , \tag{8.3}$$

where u^J_l are the nodal displacements. With the interpolations (8.3), the first of eqns. (8.2) becomes

$$\sigma_{ji} = A^J_{jil}u^J_l \ , \qquad A^J_{jil} = C^0_{jikl}S^J_{,k} + \frac{1}{r}C^0_{ji22}T^J_l \ . \tag{8.4}$$

Similarly, the vector f_i may be written as

$$f_i = B^J_{il}u^J_l \ , \qquad B^J_{il} = \begin{bmatrix} \frac{1}{r}(C^0_{00kl} - C^0_{22kl})S^J_{,k} + \frac{1}{r^2}(C^0_{0022} - C^0_{2222})T^J_l \\ \frac{1}{r}C^0_{01kl}S^J_{,k} + \frac{1}{r^2}C^0_{0122}T^J_l \end{bmatrix} . \tag{8.5}$$

Substitution of eqns. (8.4) and (8.5) into eqn. (8.1) yields the element stiffness relation for axisymmetric linear elasticity, *viz.,*

$$K^{IJ}_{il}u^J_l = f^I_i \ , \qquad K^{IJ}_{il} = \int_V (\, S^I_{,j}A^J_{jil} - S^I B^J_{il} \,)\mathrm{d}V \ , \qquad f^I_i = \int_S S^I T_i \mathrm{d}S \ . \tag{8.6}$$

9. Nonlinear Elastic Finite Element Equations

Equation (6.7) is the residual of the nonlinear system, *viz.,*

$$r^I_i = \int_V S^I_{,j}N_{ji}\mathrm{d}V - \int_V S^I f_i \mathrm{d}V - \int_S S^I T_i \mathrm{d}S = 0 \, . \tag{9.1}$$

Equation (9.1) is solved with Newton-Raphson iteration, the procedure of which is

$$J^{IJ}_{il}\Delta u^J_l = -r^I_i \ , \qquad {}^{\mathrm{imp}}u^J_l = u^J_l + \Delta u^J_l \ , \qquad J^{IJ}_{il} = \frac{\partial r^I_i}{\partial u^J_l} \ , \tag{9.2}$$

where ${}^{\mathrm{imp}}u^J_l$ is an improved guess to the nodal displacements, and J^{IJ}_{il} is the Jacobian of the system. So, differentiation of eqn. (9.1) gives the Jacobian

$$J^{IJ}_{il} = \int_V S^I_{,j}\frac{\partial N_{ji}}{\partial u^J_l}\mathrm{d}V - \int_V S^I \frac{\partial f_i}{\partial u^J_l}\mathrm{d}V \ . \tag{9.3}$$

Now, for the axisymmetric deformation, the deformation gradient is

$$F_{ij} = \delta_{ij} + u_{i,j} \ , \qquad F_{22} = 1 + \frac{1}{r}u_0 \ , \tag{9.4}$$

cf., the first of eqns. (3.1). Next, interpolate the displacement field through the element via

$$u_l = S^J u_l^J \ , \qquad u_{l,k} = S^J_{,k} u_l^J \ , \qquad u_0 = T_l^J u_l^J \ , \tag{9.5}$$

where u_l^J are the nodal displacements, and where T_l^J is defined above in the third of eqns. (8.3). Thus, putting the interpolations (9.5) into eqns. (9.4), one obtains

$$F_{lk} = \delta_{lk} + S^J_{,k} u_l^J \ , \qquad F_{22} = 1 + \frac{1}{r} T_l^J u_l^J \ . \tag{9.6}$$

Differentiation of eqns. (9.6) then yields

$$\frac{\partial F_{pq}}{\partial u_l^J} = S^J_{,q} \delta_{pl} \ , \qquad \frac{\partial F_{22}}{\partial u_l^J} = \frac{1}{r} T_l^J \ . \tag{9.7}$$

Next, we have the derivatives

$$\frac{\partial N_{ji}}{\partial u_l^J} = \frac{\partial N_{ji}}{\partial F_{pq}} \frac{\partial F_{pq}}{\partial u_l^J} + \frac{\partial N_{ji}}{\partial F_{22}} \frac{\partial F_{22}}{\partial u_l^J} \ , \qquad \frac{\partial f_i}{\partial u_l^J} = \frac{\partial f_i}{\partial F_{pq}} \frac{\partial F_{pq}}{\partial u_l^J} + \frac{\partial f_i}{\partial F_{22}} \frac{\partial F_{22}}{\partial u_l^J} \ . \tag{9.8}$$

Substitution of eqns. (9.7) into the first of eqns. (9.8) gives

$$\frac{\partial N_{ji}}{\partial u_l^J} \equiv A^J_{jil} = \frac{\partial N_{ji}}{\partial F_{lk}} S^J_{,k} + \frac{1}{r} \frac{\partial N_{ji}}{\partial F_{22}} T_l^J \ . \tag{9.9}$$

Similarly, substitute eqns. (9.7) into the second of eqns. (9.8) to obtain

$$\frac{\partial f_i}{\partial u_l^J} \equiv B^J_{il} = \begin{bmatrix} \frac{1}{r}\left(\frac{\partial N_{00}}{\partial F_{lk}} - \frac{\partial N_{22}}{\partial F_{lk}}\right) S^J_{,k} + \frac{1}{r^2}\left(\frac{\partial N_{00}}{\partial F_{22}} - \frac{\partial N_{22}}{\partial F_{22}}\right) T_l^J \\ \frac{1}{r} \frac{\partial N_{01}}{\partial F_{lk}} S^J_{,k} + \frac{1}{r^2} \frac{\partial N_{01}}{\partial F_{22}} T_l^J \end{bmatrix} . \tag{9.10}$$

Finally, with eqns. (9.9) and (9.10), the Jacobian (9.3) becomes

$$J^{IJ}_{il} = \int_V \left(S^I_{,j} A^J_{jil} - S^I B^J_{il} \right) \mathrm{d}V \ . \tag{9.11}$$

When performing the iterations, a load step was considered as being converged when all the nodal values Δu_l^J satisfied

$$\left| \Delta u_l^J \right| \le 10^{-4} \max \left| u_l^J \right| \ . \tag{9.12}$$

10. Numerical Example – Necking and Drawdown of a Uniaxial Tension Specimen

The uniaxial tension specimen analyzed is a right circular cylinder of length $2L$ and radius R, where $L = 3$ in and $R_0 = 0.25$ in. To initiate necking and drawdown, the radius of the specimen is taken as

$$R = \frac{R_0}{2} \left[2 - f - f \cos\left(\frac{\pi z}{L} \right) \right] \ , \tag{10.1}$$

with $f = 0.05$. In other words, at $z = L$, the radius is $R = R_0$, and at $z = 0$, the radius is $R = (1 - f) R_0 = 0.95 R_0$. The midplane of the specimen is located at $z = 0$, and due to symmetry, only the upper half is analyzed numerically.

The grid of nodes used is shown below in Fig. 6. The grid spans the area $r \in (0, R) \times z \in (0, L)$, and it consists of a $6 \times 181 = 1086$ array of nodes, and a $5 \times 180 = 900$ array of elements.

The boundary conditions for the problem are

$$u_r = 0 \text{ on } r = 0 \ , \qquad u_z = 0 \text{ on } z = 0 \ , \qquad u_z = U \text{ on } z = L \ . \qquad (10.2)$$

The load stepping history used is shown below in the table, where U is in inches. For the first load step 0, the initial guess to the nonlinear solution is a linear elastic solution, and then iterations are used to achieve equilibrium for the nonlinear problem. For subsequent load steps, the initial guess to the solution is the solution from the previous load step scaled to fit the boundary conditions for the current load step. Necking starts to occur around $U \approx 1.5$ in, and after that, steps of size $\Delta U = 0.1$ in were used. For this load step size, approximately 4 to 6 iterations were required to obtain equilibrium for each step.

step	0	1	2	3	4	5	6	7	8	9	10	11
U	0.5	1.0	1.5	1.6	1.7	1.8	1.9	2.0	2.1	2.2	2.3	2.4

12	13	14	15	16	17	18	19	20	21	22	23	24
2.5	2.6	2.7	2.8	2.9	3.0	3.1	3.2	3.3	3.4	3.5	3.6	3.7

25	26	27	28	29	30	31	32
3.8	3.9	4.0	4.1	4.2	4.3	4.4	4.5

Figures 7 through 9 below show the deformed grid at various load levels. Note that the Figs. 6 through 9 all possess the same scale. As Fig. 7 shows, drawdown has initiated by the time $U = 2.0$ in is reached. Figures 8 and 9, at load levels $U = 3.3$ in and $U = 4.5$ in, respectively, show the steady state propagation of the drawing.

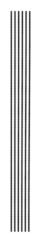

Figure 6. Undeformed tension specimen.

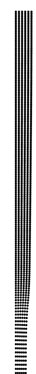

Figure 7. Tension specimen at $U = 2.0$ in.

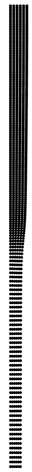

Figure 8. Tension specimen at $U = 3.3$ in.

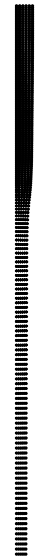

Figure 9. Tension specimen at $U = 4.5$ in.

Figures 10 and 11 below show the true strain component ε_{zz} and true stress component σ_{zz} calculated at the centers of the elements whose left boundaries are at $r = 0$. The load level is $U = 4.5$ in, and the Z–coordinate in the figures is in the undeformed configuration. The transition region between drawn and undrawn material is highly evident.

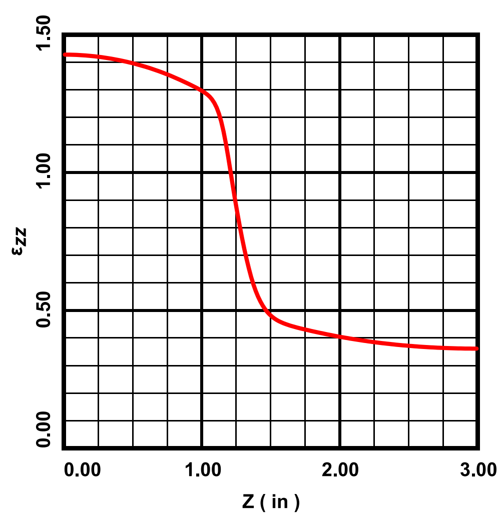

Figure 10. Strain component ε_{zz} at $U = 4.5$ in.

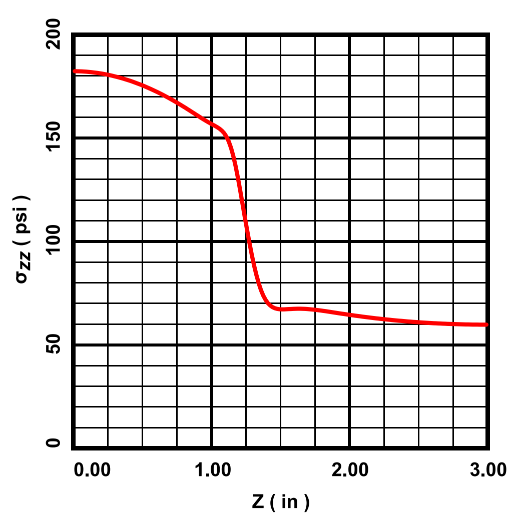

Figure 11. Stress component σ_{zz} at $U = 4.5$ in.

11. Closing Remarks

The major advantage of doing the calculations in two dimensions is that the eigenproblems in Secs. 1 through 3 are solved in closed form, which results in a highly reliable, and quickly executing, numerical method.